An Interpretation of the Aeromagnetic and Gravity Data and Derivative Maps of the Craig and Dixon Entrance 1°x3° Quadrangles and the Western Edges of the Ketchikan and Prince Rupert Quadrangles, Southeastern Alaska

By
J.C. Wynn, R.P. Kucks, and D. J. Grybeck

Digital Data Series 56

INTRODUCTION

The U.S. Geological Survey (USGS) is required by the Alaska National Interest Lands Conservation Act (ANILCA, Public Law 96-487) to survey certain Federal lands to determine their mineral resource potential. As part of continuing studies designed to fulfill this responsibility, geochemical, geological and geophysical surveys of the Craig and Dixon Entrance (CDE) 1°x3° quadrangles in southeastern Alaska were undertaken by the USGS during the summers of 1983-85, 1989, and 1991. The geochemical data have been reported by Cathrall and others (1993) and Cathrall (1994). A simplified geologic map has been compiled especially for this report based largely on the work of Eberlein and others (1983) and Gehrels (1991, 1992). Brew (1996) also produced a compilation. This report presents available magnetic and gravity data and an interpretation thereof.

GEOGRAPHIC AND GEOLOGIC SETTING OF THE CRAIG STUDY AREA

The Craig study area comprises about 1,400 mi^2 (3,600 km^2) between latitude 54°40' and 56° N. and longitude 131°50' and 134°40' W. of the southeastern tip of the Alaskan Panhandle. The CDE quadrangles (fig. 1) are located west of Ketchikan and include all but the northern tip of Prince of Wales Island as well as outlying islands to the west from Dall Island in the south to Coronation Island in the northwest. In order to integrate parts of Prince of Wales Island south of 56° N., parts of the western edges of the Ketchikan and Prince Rupert 1:250,000-scale quadrangles are included in this geophysical compilation. The largest single landmass in the Craig area is Prince of Wales Island, the southernmost major island of the Alexander Archipelago; the study area is entirely in the Tongass National Forest. The Prince of Wales Mountains are moderately glaciated mountains reaching to 3,800 ft (1,160 m). The Kupreanof Lowlands consist of islands and channels on the
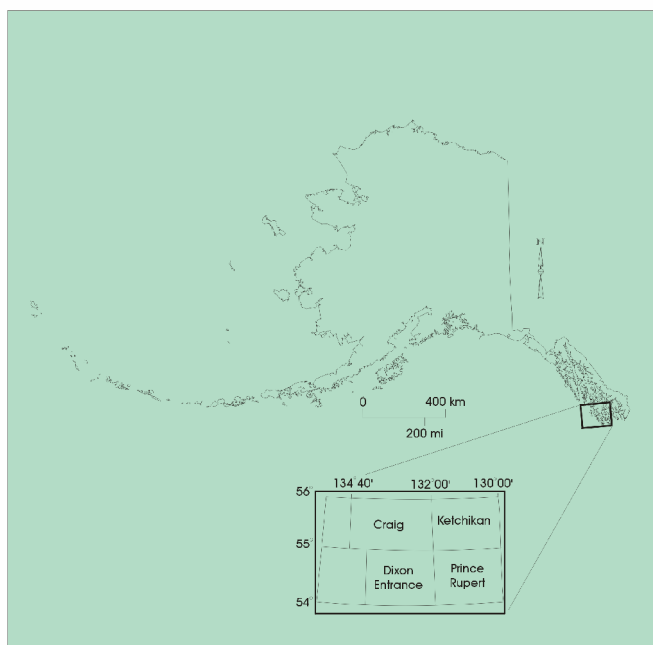

Figure 1. **Location of the Craig & Dixon Entrance quadrangles, southeastern Alaska.**

western side of Prince of Wales Island; maximum elevation is about 3,000 ft (915 m). The Coastal Foothills consist of blocks of high mountains on the east of Prince of Wales Island extending to 4,500 ft (1,372 m) elevation.

The CDE area contains parts of two northwest-trending tectono-stratigraphic terranes separated by a similarly trending overlap assemblage (from southwest to northeast): the Alexander Terrane, the Gravina-Nutzotin overlap assemblage, and the Taku terrane (Monger and Berg, 1987; Warhaftig, 1965). A simplified geologic map of the study area compiled by Don Grybeck is included in this CD-ROM as the underlying base for some of the large images representing the geophysical data.

PREVIOUS GEOPHYSICAL WORK

Aeromagnetic surveys were flown in parts of the CDE area as early as 1945 (Rossman and others, 1956; Decker, 1979) at 1-mi spacings and at elevations ranging from 500 to 6,000 ft above mean sea level. Unfortunately, they covered only parts of the eastern Craig quadrangle and only the southeastern tip of Prince of Wales Island. The 1945 data are not digitally recoverable. A digital aeromagnetic survey flown in three parts during 1978 (USGS, 1984) covered all of the land and much of the water of the CDE area and has been merged and compiled into one map with derivative products as part of this report. A limited-scale helicopter-borne spectral radiometric survey was also carried out in 1978 but covered primarily the previously identified Bokan Mountain uranium occurrences and surrounding terrane in southern Prince of Wales Island (Burgett and Krause, 1979). Initial gravity data were acquired in 1968-69 by using paired altimeters and tide tables for elevation control (Barnes, 1972; Barnes and others 1972a, b). These data were supplemented with additional helicopter-acquired gravity stations obtained during the summers of 1984- 85 and 1991 and are assembled together for the first time in this report. The study area includes all of the CDE 1:250,000-scale quadrangles and a small part of the western edges of the Ketchikan and Prince Rupert 1:250,000-scale quadrangles (fig. 1).

GRAVITY DATA

Data Acquisition, Reduction, and Compilation

Gravity data acquisition in the CDE area began in 1968, using early 0.1-mGal sensitivity LaCoste-Romberg gravimeters. Elevation control was obtained by using paired altimeters and tide tables (Barnes, 1972; Barnes and others, 1972b, 1977). Most of the gravity stations were around the coastal margins of Prince of Wales and some outlying islands. Denser station spacing was implemented during 1984-85 and 1991 by using skiffs and helicopter support to fill in the interior of Prince of Wales Island and some of the other outlying islands. These data were reduced to the simple Bouguer anomaly by using elevation control from three Wallace & Tiernan[1] altimeters calibrated against known elevations at the beginning and at the end of each base-station loop. Barometric pressures obtained from the National Weather Service for Ketchikan were used to improve interpolated elevations between base station readings. The complete Bouguer anomaly (CBA) for each measurement was calculated by using edited digital elevation data acquired from the Department of Defense to remove the effects of topographic relief. Data and further information on global topography at 30' grid spacing can be obtained at several World Wide Web sites (U.S. Geological Survey, 1997). The CBA map is viewable in the "\images" directory. The isostatic residual anomaly (ISO) was calculated by using USGS digital topographic data and digital bathymetry obtained from Oregon State University (Simpson and others, 1983). Data and more information on available sea-floor bathymetry can be obtained from Smith and Sandwell (1997). The use of ISO gravity should theoretically remove the effects of isostatic disequilibrium associated with the continental-crust-oceanic-margin transition; its effect is to shift anomalies so that they more precisely overlay their causative source bodies. The reasons and methodology behind isostatic corrections to gravity data has been given by Blakely (1995). The ISO map is viewable in the "\images" directory in several different forms, including draped as color over a shaded-relief topographic image and as contours superimposed on the simplified geologic map.

---

[1] Reference to any specific commercial product, process, or service by trade name, trademark, manufacturer, or otherwise does not constitute or imply its endorsement, recommendation, or favoring by the United States Government or any agency thereof.

Complete Bouguer Anomaly versus Isostatic Residual Anomaly Gravity

We present two different versions of the gravity data in this CD-ROM: the complete Bouguer anomaly (generally abbreviated CBA) and the isostatic residual anomaly (ISO). The CBA represents the observed gravity field for a given station, with corrections added in for instrument drift, diurnal variation caused by the Sun and the Moon, latitude (the oblateness of the Earth's surface), and density of the rock lying between the station and sea level. These factors in aggregate give the Bouguer anomaly. Adding corrections for topographic effects then gives the CBA. These topographic corrections are made by using a digital topographic model to calculate the effects of mass contributions (from nearby mountains) or lack thereof (from voids caused by nearby valleys) owing to the physical relief that surrounds the gravity station. These calculations are carried out to a distance of 167 km from the station, and a compensation is added to the corrected gravity value. These corrections and adjustments have been explained in greater detail by Blakely (1995).

Continents and ocean basins represent mass concentrations and deficiencies, respectively, and typically have large lateral dimensions. Deep underlying masses provide natural compensation for topographic loads, not unlike ice cubes floating in a glass of water. This type of compensation is known as isostatic. The CDE quadrangles are located on a continental-oceanic margin. There is ample reason to believe that isostatic compensation effects in these regions would be nontrivial; simply compare the CBA and. the ISO anomaly maps. Usually, the anomalies caused by the compensating masses are long in wavelength and correlate inversely with long-wavelength attributes of topography. In general, large mass concentrations and mass deficiencies are compensated for at depth to first order, so that total mass in each vertical section of a gravity profile is laterally uniform. Small, higher order transition effects, however, are apparent when CBA and ISO gravity maps in the CDE quadrangles are compared: gravity anomalies shift and stretch perpendicular to the direction of the ocean-margin axis. These two different maps are shown in several different forms in the "\imagery" directory.

When our digital terrain model (meshed with a digital bathymetry model) is used, it is a relatively straightforward procedure to estimate the shape of the crust-mantle interface consistent with the Airy model for isostatic compensation and calculate at each observation point the gravitational effect of the volume (Jachens and Roberts, 1981; Simpson and others, 1983).

The significant difference observable between the CBA anomaly map and the ISO anomaly map makes it clear that, in CDE area, isostatic compensation is significant; therefore, the ISO map is the gravity map of choice. In such a transition zone, we can reasonably expect that the correlation between mapped geology and gravity anomalies will be higher if we work with the isostatic gravity anomaly map and not the CBA map. The longer wavelength anomalies (the larger, smoother features) in the ISO map generally represent large bodies at depth--typically, large blind intrusives and plutons. The shorter wavelength anomalies (the smaller, sharper features) tend to correlate best with surface geology, especially in the isostatic gravity map.

Sedimentary rocks have relatively low densities (typically 1.5-2.5 g/cm^3), whereas igneous rocks generally have greater densities (typically 2-3.5 g/cm^3). Thus, igneous rocks have a relatively higher "weighting" in these maps, as the rather high degree of correlation between mapped intrusive bodies and the isostatic gravity anomalies shows. The overall effect is that we see relatively little correlation between anomalies and offsets in the isostatic anomaly map and any sedimentary rock units, unless there is a substantial contrast between, say, a dense shale and a relatively porous sandstone. Another example occurs when we are trying to distinguish Descon flows from clastics; the flows will generally be denser than the clastics and should show up as an increase in the strength of the ISO field in an area where there is a transition from flows to clastics. There is a significant limitation to this claim, however: we can distinguish transitions only if there is sufficient data to show clearly a transition in the first place. With few exceptions, the gravity data coverage in the CDE area is sparse, and detailed profiles would have to be acquired before we could map such transitions.

Interpretation of Specific Gravity Anomalies of Interest

The character of the gravity map is somewhat different from that of the magnetic map, in large part because the resolution of the data is coarser owing to limits on helicopter access during our surveys. Nevertheless, there are some excellent correlations between the magnetic maps and the gravity maps as well as several differences that allow us to break up certain

intrusives into discrete and substantially different components that seem, in the magnetic data, to be a single feature. The following discussion is keyed to the isostatic gravity map.

The gravity amplitude indicates that the Union Bay complex and the small islands to the northwest of it must be dense bodies, something to be expected for a zoned mafic-ultramafic body (though serpentinization often reduces the aggregate density); the correlation with the magnetic image is very good considering the lack of gravity stations in Clarence Strait (the deep channel between Union Bay and Prince of Wales Island).

There is also a good correlation between magnetic and gravity data for the Kasaan Peninsula and the rocks to the northwest of the peninsula. The magnetic data would seem to imply that the Kasaan Peninsula is separate, whereas the gravity would seem to imply that it is a continuation of the exposed rocks to the northwest. This apparent continuity is probably an artifact of the coarser gravity station density and the resultant poorer resolution of the gravity map. Interestingly, the Salt Chuck ore body lies on the southeastern edge of the highest part of the gravity anomaly and the coincident magnetic anomaly. The implication is that the rest of the margins of this coincident geophysical anomaly on the northwestern end of the Kasaan Peninsula hold significant potential for similar deposits.

The cryptic Twin Mountain-Staney Creek magnetic anomaly (see model in fig. 2) shows up in the gravity map as a broad gravity high. If not for the magnetic data, the source would be interpreted as a large buried and homogeneous pluton; instead, we feel it is a composite pluton composed of several different intrusives.

The higher isostatic gravity values west of Hecate Island are probably a direct consequence of an underlying oceanic crust. Station density does not permit a more detailed characterization, and the intrusives seen in the magnetic data over Warren and Coronation Islands cannot be resolved in the coarser gravity data.

This summary of the gravity anomalies encountered in the CDE area is very abbreviated and does not address a number of important issues, including the depth to the crust below Prince of Wales Island. Because of the sparsity of gravity stations and time constraints on the release of these data, further analysis and modeling are probably not warranted at this time. The authors have been given access to density data collected by Dave Barnes in the late 1960's and early 1970's, however. These densities could be compared with the new geologic map included in this report to determine ranges of densities for given lithologies. Normally, there is quite a bit of

Figure 2. Model of the source of the Twin Mountain gravity and magnetic anomalies.

variability in the densities and magnetic susceptibilities of rock units, because there are many variables involved (including local hydrothermal alteration) that can modify these values. Nevertheless, if additional, more closely spaced gravity stations are acquired along profiles, these densities could prove useful in more detailed modeling. The "/Data" folder of this report includes a simplified version of the sample-density database assembled by Dave Barnes, called "CDE-Densities.txt" (Dave Barnes, USGS, written communication, 1984).
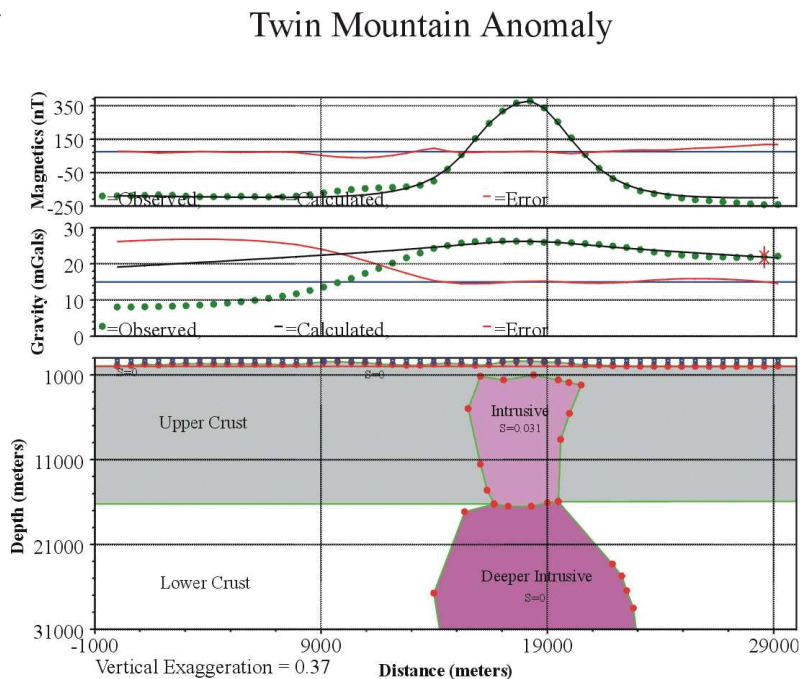
4

AEROMAGNETIC DATA

Data Acquisition and Processing

During August and September 1982, Diversified Technology Corporation (under contract to the U.S. Geological Survey) flew three airborne magnetic surveys draped over the topography in the CDE area (U.S. Geological Survey, 1984). The data are summarized in table 1, where 1000' AG means the aircraft draped the topography at 1000 ft (305 m) mean terrain clearance. These datasets were combined and then processed to remove the International Geomagnetic Reference Field (IGRF) for 1982. The resulting residual magnetic data ("Resid") are shown in the "\images" directory. Several derivative and filtered products were developed digitally in order to enhance the data to aid in geologic interpretation; one of these steps was reduction-to-the-pole ("RedPole"), whereby asymmetry caused by nonpolar geomagnetic latitude was removed. The result is an image in which anomalies should lie over their sources. This RedPole map is shown in the "\images" directory in several different forms, including draped as color over a shaded-relief topographic image and as contours superimposed on the simplified geologic map. More information and data about magnetic data in Alaska have been given by Saltus and Simmons (1997).

TABLE 1. Recent aeromagnetic surveys of the Craig-Dixon-Entrance quadrangles
[IGRF, International Geomagnetic Reference Field]

No.	Name	Spacing (mi/km)	Direc-tion	Altitude	Max-Lat.	Min-Lat	Max-Long	Min-Long	Line (km)	IGRF model
1	Craig	1.0/ 1.6	N-S	1000' AG	56.03	54.63	133.83	131.83	5730	IGRF75
2	N W Craig	1.0/ 1.6	E-W	1000' AG	56.00	55.83	134.50	133.25	630	IGRF75
3	S Craig	1.0/ 1.6	N68E	1000' AG	54.95	54.67	132.75	132.20	350	IGRF75

Residual Magnetic Field versus Reduced-to-the-Pole Magnetic Field

In much the same way that distinctions made between CBA and ISO gravity, there have also been shape- shifting compensations performed on the magnetic data. The raw magnetic data were delivered to the USGS by the contractor after correcting and compensating for several forms of time-varying noise. One of these forms is instrumental drift; another is diurnal drift; a third is a tie-line or leveling correction. A fourth correction compensates for the fact that there is a slow, steady westward drift of a second-order component of the Earth's dipolar field. The time scale here is measured in years. Instrumental drift is self-explanatory; diurnal (daily) drift is caused by the Earth's rotation within a complex geomagnetic field, some of the components of which are asymmetric with respect to the direction of the Sun (caused by the buffetings of the solar wind). The leveling or tie-line correction simply forces the field to be consistent for a given elevation above ground, despite the fact that the acquisition aircraft inevitably varies its altitude during the survey. The fourth correction compensates for the shifting nature of the Earth's magnetic field; the actual correction process is described as "removal of the IGRF." The residual magnetic field that results from all these corrections can thus be compared with confidence to other magnetic surveys acquired in different years. We use the term "residual magnetic field" because it is the field that remains after all the drift effects are taken out.

In preparing this CD-ROM we have added RedPole as a fifth correction. The magnetic anomaly over a given source body is asymmetric with respect to that body because of the nonvertical direction of the Earth's magnetic field vector; in North America this field vector has an inclination ranging between 40º and 60º from the horizontal and a declination (i.e., the difference in compass direction between magnetic field lines and true north) of up to 15º. Consequently, hand-held compasses do not generally line up pointing toward true north, and contour plots of magnetic anomalies do not line up over their source or causative bodies. We can and have mathematically corrected for this failing, however (see, for example, the work of Blakley, 1995); the result is the RedPole magnetic field, which now has magnetic highs (and in some cases lows)

mostly positioned directly over the source or causative bodies. We can use either the residual magnetic field or the RedPole field to model the source bodies in three dimensions, but the RedPole map in general correlates more closely with mapped geology. For the same reasons that we generally prefer not to use the CBA gravity map, we generally avoid using the residual magnetic anomaly map when we have a significant inclination and declination in the Earth's magnetic field vector. Simply put, the representation of the geology given by the RedPole map is much better on casual examination than that given by the residual map. In cases where sources are buried or where there is extensive vegetative or water cover, the RedPole magnetic map (and sometimes the ISO gravity map) allows us to confidently extend specific map units beneath sediment and water cover.

Magnetic Depth to Source

Euler deconvolution is one method for calculating depth to source from magnetic data (Blakely, 1995). On an experimental basis, Euler deconvolution calculations were made from the CDE magnetic data. Results are shown in figure 3 and in two files in the "\images" directory for two different structural indexes. The example in figure 3 shows an example for a structural index (SI) of 1 (explained below). In this representation, the smaller circles represent shallower sources and larger circles represent deeper sources; dips and strikes of three-dimensional features can be readily observed by how the circles lie one atop another. The features utilized for the calculations are gradients and offsets in the magnetic data. For this calculation, an SI of 1 (shown here) emphasizes intrusions, dikes, and fault-caused features; for this reason, not all of the magnetic gradients in the RedPole image are strongly represented. An SI of 2 emphasizes cylindrical source objects; this figure is also included in the "\images" directory and is significantly different from figure 3. In this other image, the major
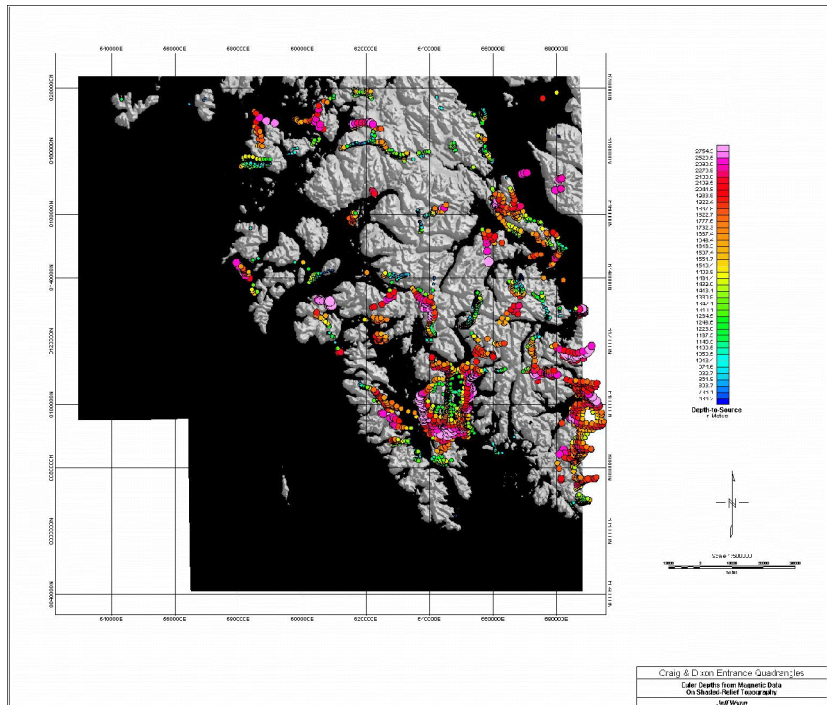

Figure 3. Euler deconvolution solutions (depth-to-magnetic-source) for the Craig & Dixon Entrance quadrangles.

intrusions in the CDE quadrangles stand out much more sharply. From figure 3, on the other hand, a geologist can readily identify lithologic contacts and get a sense of how deep the causative rocks are; in some cases, we can even see the dip of the contact. Because of the limited data window, we cannot use Euler deconvolution to obtain the thickness of the crust from these data. The isostatic correction algorithm discussed earlier in the gravity section utilizes gravity data, bathymetry, and topography from the CDE and well beyond to compensate for the changing thickness of the crust in the narrower CDE area.

Interpretation of Specific Magnetic Anomalies of Interest

A brief overview of the magnetic map follows. This discussion is keyed to the RedPole map ("CDE-AnnotatedMagAnomalyMap.jpg" in the "\images" directory), beginning in the northeast. Coordinates in the following text are UTM, keyed to figure 4. In Union Bay, a strong, vertical-cylinder magnetic anomaly overlies the Union Bay Intrusive. This anomaly is unusually strong; in fact, airline navigation maps even warn pilots to expect large deviations in their compass headings in the vicinity. While acquiring a gravity station in this location, two of us (JCW and DJG) observed 5-cm-thick veins of magnetite in several exposures.

A continuous high magnetic anomaly covers all of the Kasaan Peninsula but also extends across Kasaan Bay to include Clover Mountain to the south. The character of the anomaly, however, changes as it crosses Kasaan Bay. In the north, over the Kasaan Peninsula, the mag anomaly displays relatively long wavelengths, whereas, south of the bay, amplitudes are higher and wavelengths are somewhat shorter, suggesting that the anomalies from two different sources are merging. The Kasaan Peninsula is mapped primarily as gabbros and monzonite intrusives. The rocks underlying the Clover Mountain magnetic anomaly are Descon (SOg) sediments, implying that the source rocks for the magnetic anomaly must lie (relatively shallowly) buried beneath a Descon layer. Note the previous discussion of the relationship of the economically important Salt Chuck mine with the edge of a coincident magnetic and gravity high located in the northwestern corner of the Kasaan Peninsula.
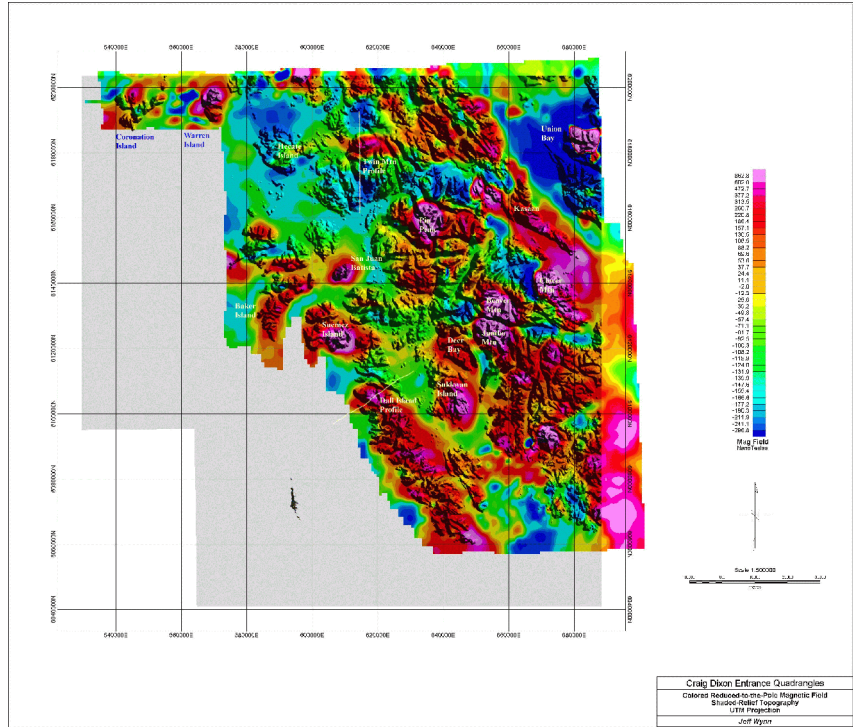

Figure 4. The annotated reduced-to-the-pole magnetic anomaly map of the Craig & Dixon Entrance quadrangles.

An unexpected magnetic high underlying Twin Mountain (roughly 615000E. by 618000N.), trending roughly east-west. It is unexpected because the underlying geology is sedimentary. The magnetic anomaly extends from central Hecate Island in the west to Staney Creek in the east. The area is underlain by Hecate Limestone, Karheen Formation (Dk) sediments, and sedimentary rocks of the Staney Creek and Tuxekan Passage area (DSs). USGS geologists have seen scattered rhyolite and andesite flows and even small plugs of andesite, dacite, and diorite elsewhere in the Karheen Formation.

This magnetic anomaly appears to map the presence of a major blind intrusive (see computed model in fig. 2). The modeled intrusive does not quite breach the surface but must reach to within a kilometer. These data are unusual in that the shorter wavelength shape of the magnetic anomaly suggests a much shallower source than the broader shape of the gravity anomaly (they are both modeled simultaneously here). In order to model the two together, we were forced to invoke a two-phase intrusive body with a shallow, more magnetic component and a deeper, more dense part of the intrusive below about 13,500 m. This intrusive is significant in that it may imply an undiscovered Cu-Pd mineral resource potential due to the spatial connection of this anomaly to the magnetic anomaly over the Salt Chuck deposit to the immediate east (Gault and Wahrhaftig,1992; Loney and Himmelberg, 1992; Watkinson and Melling, 1989).

Another magnetic high underlies Warren Island, but this is no surprise because the island is mapped as Descon sediments intruded by Cretaceous intermediate plutonic rocks, some of which crop out and have moderate to strong magnetic susceptibility as hand samples. Not surprisingly, the areal extent of the pluton beneath the island and the surrounding sea is more than twice the island exposure.

Coronation Island is mapped as roughly 95 percent Descon sediments and Hecate Limestone, but two tiny exposures of Cretaceous intrusive rock in the northern and central part of the island suggest that most of the island is underlain by intrusive rock. It is possible that there are up to four separate but probably related intrusive bodies underpinning the island (this assumption is based on the overlapping but apparently discrete anomalies observed).

San Juan Batista Island correlates closely with a magnetic anomaly similar to the one observed at Warren Island, but it appears to be connected to the west and southwest to a long arcuate anomaly beneath Baker Island, most of which is covered

by Descon sediments. In the southeast and on the southern tip of Baker Island, more Cretaceous intrusive rocks are exposed, and the magnetic data suggest that a subsurface pluton is continuous from San Juan Batista to the southwestern tip of the island (Cape Bartolome). A (probably) separate anomaly lies over the part of the immediately adjacent westward island (Lulu Island), centered where another Cretaceous stock is partially exposed, but the anomaly extends under the sea to the west.

A strong magnetic high lies over Suemez Island. Where it is strongest in the southeastern part of the island, it is underlain by another Cretaceous pluton. The magnetic signature suggests two things here: (1) the entire island is underlain by a small pluton, and (2) this pluton is distinct and different, despite its proximity, from the huge pluton underlying all of Dall Island.

A major surprise in the magnetic data is the extensive magnetic anomaly associated with Dall Island. This island is covered by Hecate Limestone, Descon sediments, and magnetically inert Wales Group metasedimentary rocks, along with tiny bits and pieces of exposed intrusive rock (Kg). A profile that we modeled across the Dall Island magnetic anomaly (fig. 5) suggests that the Cretaceous pluton causing the anomaly may be substantial and rises to within a kilometer of the ground surface beneath and slightly to the northeast of the topographic high marking the island ridge.

Gravity data in this southwestern area are inadequate for us to model the gravity component also; in fact, the magnetic coverage is truncated to the immediate west of Dall Island, an indication that the western boundaries of the model are poorly constrained. The fact that the tonalite and other components of the Kg unit are commonly magnetic suggests to us that Dall Island is underlain by a large pluton. The upper sedimentary rocks are exposed because they were uplifted by the emplacement of this pluton. The depth to the bottom of the pluton cannot be defined with available data. Normally, the bottom of a magnetic source is poorly defined because of the dominance of the upper surface of the source object on the data. The Curie

Figure 5. Model of the source for the magnetic anomaly lying over northern Dall Island.

temperature for magnetite is about 580ºC (Blakley, 1995). At depths below where this temperature is reached (the Curie isotherm, anywhere from 10-25 km, depending on the geothermal regime) (Stacey, 1969), there is no further contribution by the source body to the magnetic anomaly, even though the body may reach deeper. Because we have only limited gravity data around Dall Island, the bottom of the intrusive in figure 5 cannot be defined and is drawn arbitrarily.
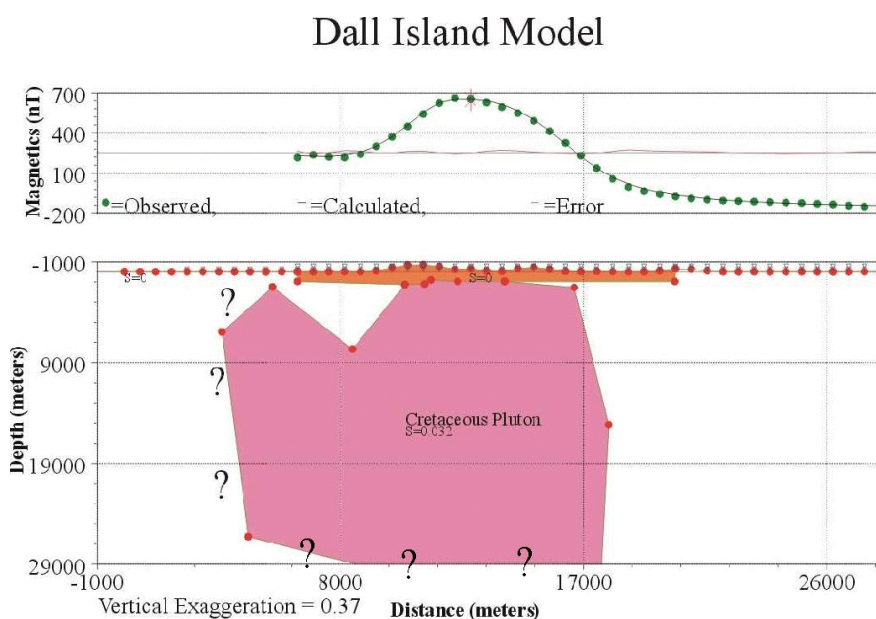
The large magnetic anomaly underlying Dall Island substantially increases the possibility of a significant mineral resource potential for this island, in part because fluids associated with the later intrusive event have invaded and altered the sediments. We have also mapped mineralized quartz veins at the southern tip of Dall Island (at a locality called McCloud Bay) and believe that these veins are pluton related. Mineralization has also been reported at several places along the western side of the island-- e.g., at Grace Mountain farther north (see the Dixon Entrance digital topographic map included in the "\images" directory. There may be other sites where mineralizing fluids have escaped into overlying sediments, giving rise to undiscovered skarns and massive sulfide/epithermal vein deposits, among other things.

A roughly north-oriented magnetic anomaly at Sukkwan Island suggests that the exposed syenite in the southeastern part of the island may underlie the entire island and also may extend across Sukkwan Strait to Eek Lake all the way north to Deer Bay on the main body of Prince of Wales Island. In the magnetic data, it is not clear if the strong Jumbo Mountain magnetic anomaly is just an extension of the Sukkwan syenite, but the gravity data (discussed below) make it clear that they are

separate; thus, any economic potential associated with this particular magnetic anomaly is restricted to the Jumbo Mountain side of the strait.

A large magnetic anomaly encompasses Jumbo Mountain and extends north across Sulzer Portage to Beaver Mountain. Although magnetic data seem to indicate that Cretaceous plutons mapped on both mountains are continuous, gravity data show that they are not. A gravity high at Beaver Mountain contrasts with a gravity low at Jumbo Mountain, with a sharp gradient at Sulzer Portage-Cholmondely Sound. This gradient is important in any mineral resource estimate because the Jumbo Mine has produced substantial amounts of copper and gold. The gravity data are consistent with a major east-west fault separating the two plutons; more likely, they are different intrusive events having different compositions. Thus, Beaver Mountain may not have the same economic potential as Jumbo Mountain.

SUMMARY

On this CD-ROM we are releasing USGS-acquired geophysical data for CDE 1:250,000-scale quadrangles of southeastern Alaska. Much of the data have never appeared before in the public domain, including a simplified geologic map, the raw gravity and magnetic data, and derivative products including depth-to-source images, various grids of the data, imaging representations, rock densities, and overlays of the data. In addition, we have added a limited interpretation of what the gravity and magnetic data indicate about the underlying geology, structures, and their relationship to known and potential hidden mineral resources. This interpretation is necessarily limited in the case of the gravity data by the general sparsity of stations. For convenience, we have also included here various representations of the digital topography as well as USGS topographic images, including the raw, original form of the digital topography and the digital raster graphics images of the topographic maps also available on U.S. Geological Survey Web site http://agdc.usgs.gov/data/usgs/geodata/ .

The magnetic and gravity data released here cover all of the CDE quadrangles as well as the westernmost portions of the Ketchikan and Prince Rupert quadrangles, up to 56º N. latitude. Combining magnetic and gravity data allows us to resolve ambiguities in subsurface structural interpretation that would be unresolvable if only one or the other dataset was used by itself. Several "blind" intrusives and plutons have been recognized, and two of these have been modeled. Known mineral deposits and prospects are now placed in the context of the subsurface geology influencing and moderating their emplacement.

DISCLAIMERS

This Compact Disc-Read Only Memory (CD-ROM) publication was prepared by an agency of the United States Government. Neither the United States Government nor any agency thereof, nor any of their employees, makes any warranty, expressed or implied, or assumes any legal liability or responsibility for the accuracy, completeness, or usefulness of any information, apparatus, product, or process disclosed in this report, or represents that its use would not infringe privately owned rights. Reference therein to any specific commercial product, process, or service by trade name, trademark, manufacturer, or otherwise does not necessarily constitute or imply its endorsement, recommendation, or favoring by the United States Government or any agency thereof.

Although all data and software published on this CD-ROM have been used by the USGS, no warranty, expressed or implied, is made by the USGS as to the accuracy of the data and related materials and (or) the functioning of the software. The act of distribution shall not constitute any such warranty, and no responsibility is assumed by the USGS in the use of this data, software, or related materials.

ACKNOWLEDGMENTS

REFERENCES CITED

Barnes, D.F., 1972, Summary of operational reports of a preliminary gravity survey of southeastern Alaska [sixteen 1:250,000 simple Bouguer gravity anomaly maps of southeastern Alaska showing station locations, anomaly values, and generalized 10-milligal contours]: U.S. Geological Survey open-file maps, 16 sheets.

Barnes, D.F., Olson, R.C., Holden, K.D., Morin, R.L., and Erwin, M.J., 1972a, Tabulated gravity data from southeastern Alaska obtained during the 1968 field season: U.S. Geological Survey Open-File Report, 76 p.

Barnes, D.F., Popenoe, Peter, Olson, R.C., McKenzie, M.V., and Morin, R.L., 1972b, Tabulated gravity data from southeastern Alaska obtained during the 1969 field season: U.S. Geological Survey Open-File Report, 75 p.

Barnes, D.F., 1977, Bouguer gravity map of Alaska: U.S. Geological Survey Geophysical Investigations Map GP-913, scale 1:2,500,000.

Blakely, R.J., 1995, Potential theory in gravity and magnetic applications: New York, Cambridge University Press, 441 p. (reprinted 1996).

Brew, D.A. (compiler), 1996, Geologic map of the Craig, Dixon Entrance, and parts of the Ketchikan and Prince Rupert quadrangles, southeastern Alaska: U.S. Geological Survey Map MF-2319, scale: 1:250,000, 2 sheets, 58-p. pamphlet.

Burgett, W.A., and Krause, K.J., 1979, Helicopter-assisted radiometric survey of the Dixon Entrance quadrangle, Alaska: Grand Junction, Colo., Bendix Field Engineering Corp., U.S. Department of Energy Report GJBX-019 (79), 6 p.

Cathrall, J.B., 1994, Geochemical survey of the Craig area, Craig and Dixon Entrance quadrangles and the western edges of the Ketchikan and Prince Rupert quadrangles, Alaska: U.S. Geological Survey Bulletin 2082, 52 p., 1 plate, 7 tables.

Cathrall, J.B., Arbogast, B.F., VanTrump, George, Jr., and McDanal, S.K., 1993, Geochemical maps showing the distribution of selected elements in stream-sediment samples for the Craig, Dixon Entrance and western edges of the Ketchikan and Prince Rupert quadrangles, southeast Akaska: U.S. Geological Survey Miscellaneous Field Studies Map MF-2217-A, scale 1:250,000, 2 sheets.

Decker, John, 1979, Preliminary aeromagnetic map of southeastern Alaska, U.S. Geological Survey Open-File Report 79-1694, 1:1,000,000 scale.

Eberlein, G. D., Churkin, Michael, Jr., Carter, Claire, Berg, H. C., and Ovenshine, A. T., 1983, Geology of the Craig quadrangle, Alaska: U.S. Geological Survey Open-File Report 83-91, 52 p.

Gault, H. R., and Wahrhaftig, C., 1992, The Salt Chuck copper-palladium mine, Prince of Wales Island, southeastern Alaska. U.S. Geological Survey Open-File Report 92-293, 24 p., 5 maps.

Gehrels, G. E., 1991, Geologic map of Long Island and southern and central Dall Island, southeastern Alaska: U.S. Geological Survey Map MF-2146, 1 sheet, scale 1:63,360.

——— 1992, Geologic map of southern Prince of Wales Island, southeastern Alaska: U.S. Geological Survey Miscellaneous Investigations Series Map I-2169, 23-p. pamphlet, 1 sheet, scale 1:63,360.

Jachens, R. C., and Roberts, C. W., 1981, Documentation of a FORTRAN program, 'Isocomp', for computing isostatic residual gravity: US Geological Survey Open-File Report 81-574, 26 p.

Loney, R. A., and Himmelberg, G. R., 1992, Petrogenesis of the Pd-rich intrusion at Salt Chuck, Prince of Wales Island: An early Paleozoic Alaskan-type ultramafic body: Canadian Mineralogist, v. 30, p. 1005-1022.

Monger, J.W.H., and Berg, H.C., 1987, Lithotectonic terrane map of western Canada and southeastern Alaska, U.S. Geological Survey Map MF 1874-B, scale 1:2,500,000.

Rossman, D.L., Henderson, J.R., and Walton, M.S., Jr., 1956, Reconnaissance total-intensity aeromagnetic map of the southern part of Prince of Wales Island, Alaska: U.S. Geological Survey Geophysical Map GP-135, 1:125,000 scale.

Saltus, R.W., and Simmons, G.C., 1997, Composite and merged aeromagnetic data for Alaska: A Web site for distribution of gridded data and plot files: U.S. Geological Survey Open-File Report 97-520, 14 p. Also at http://minerals.cr.usgs.gov/publications/ofr/97-520/alaskamag.html

Simpson, R. W., Jachens, R. C., and Blakely, R. J., 1983, AIRYROOT: A FORTRAN program for calculating the gravitational attraction of an Airy isostatic root out to 166.7 km: US Geological Survey Open-File Report 83-883.

Smith, W.H.F., and Sandwell, D.T., 1997, Global seafloor topography from satellite altimetry and ship depth soundings: Science, v. 277, p. 1956-1962.

    Also at http://topex.ucsd.edu/marine_grav/mar_grav.html

Stacey, F.D., 1969, Physics of the Earth: New York, John Wiley, 324 p.

U.S. Geological Survey, 1984, Aeromagnetic map of the Craig area, Alaska: USGS Open-File Report 84-666, 1:250,000 scale, 3 sheets.

U.S. Geological Survey, 1997, GTOPO30 Global 30 arc second elevation data set: Available at http://edcwww.cr.usgs.gov/landdaac/gtopo30/gtopo30.html

Warhaftig, Clyde, 1965, Physiographic divisions of Alaska: U.S. Geological Survey Professional Paper 482.

Watkinson, D. H., and Melling, D. R., 1989, Genesis of Pd-Pt-Au-Ag-Hg minerals in Cu rich sulfides: Salt Chuck mafic-ultramafic rock complex, Alaska [abs.]: Geological Association of Canada and Association of Canada Annual meeting, Montreal, 1989, Program with Abstracts, v. 14, p. A48.